

Low-Noise Photodiode-Amplifier Circuit

Kalevi Hyyppä and Klas Ericson

Abstract—A photodiode-amplifier circuit with the photodiode in the feedback path is presented. It is named the PIF-circuit. No resistor is needed at the amplifier input to provide a path to ground for the signal and leakage currents from the photodiode and the amplifier input bias current. Therefore, one potentially dominating noise source is eliminated. At frequencies below 10 kHz, the implemented PIF-circuit has an NEP $\approx 3 \text{ fW}/\sqrt{\text{Hz}}$.

I. INTRODUCTION

COMMON photodiode-amplifier circuits have a resistor connected to the amplifier input [1], [2]. The resistor functions as a load element for the photodiode or as a feedback element for the amplifier. The resistor also provides the necessary dc-path to ground for signal and leakage currents from the photodiode and bias currents from the amplifier input. The thermal noise contribution from the resistor decreases with increasing resistance. A limit of resistance is set by the allowed amplifier output offset voltage produced by the dc-current at the amplifier input. The bulkiness, the fragility, and the microphony of a high-resistance resistor make it less suitable in certain application areas, e.g., space instrumentation.

In the circuit proposed in this brief paper, the resistor is eliminated by placing the photodiode in the feedback path. The circuit has been given the acronym PIF, from *Photodiode In Feedback*. The outstanding feature of the PIF-circuit is its ability to detect weak light or radiation pulses. The gain of the circuit is dependent on background light or radiation, making it less suitable in applications where good linearity is a requirement.

An implementation of the PIF-circuit, discussed below, is designed to detect pulses with pulse lengths in the interval 0.1–1 ms. The circuit models to be presented have been chosen to be valid in the frequency band 10 Hz–100 kHz.

II. THE PIF-CIRCUIT

The gate current of an FET and the dark current of a photodiode are of the same nature—they are both leakage currents in reverse biased p–n junctions. With proper selection of devices and bias voltages, the currents can be made equal. The correct bias can be achieved automatically by placing the photodiode in the feedback path of an operational amplifier with FET's in the input stage. This is the PIF-circuit. Its circuit diagram is shown in Fig. 1.

The PIF-circuit output voltage is coupled to the photodiode through a feedback network. It enhances the high-frequency

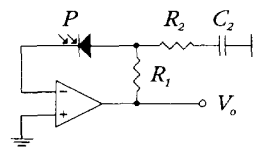


Fig. 1. The PIF-circuit. The feedback network (R_1 , R_2 , and C_2) enhances the high-frequency gain of the PIF-circuit.

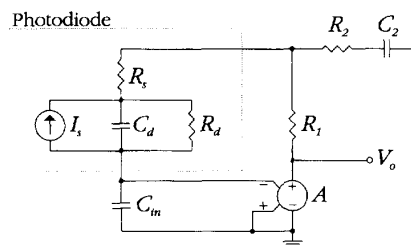


Fig. 2. Small-signal equivalent model of the PIF-circuit. The photodiode is represented by the photocurrent generator I_s , the capacitor C_d , and the resistors R_d and R_s . The input capacitance of the operational amplifier is represented by C_m .

gain of the circuit which otherwise would be too low due to the pole created by the photodiode capacitance and resistance.

III. SMALL-SIGNAL ANALYSIS

A. Transfer Function

A linear small-signal model of the PIF-circuit is shown in Fig. 2. The photodiode is represented by the photocurrent generator I_s , the capacitor C_d , the parallel resistor R_d , and the series resistor R_s .

The operational amplifier in the PIF-circuit is represented by the input capacitor C_m and a controlled voltage generator. A first-order expression is used for the transfer function of the controlled voltage generator

$$A(s) = \frac{A_0}{1 + s\tau_0} \quad (1)$$

where A_0 denotes the low-frequency voltage gain of the operational amplifier, τ_0 denotes the time constant of the transfer function, and s denotes complex angular frequency.

The transfer function from photocurrent to output voltage for the PIF-circuit becomes

$$H_{PIF}(s) = \frac{R_d(1 + s\tau_1)}{(1 + s\tau_2)(1 + s\tau_3)(1 + s\tau_d)} \quad (2)$$

where $\tau_1 = R_1C_2$, $\tau_2 = R_2C_2$, $\tau_3 = \tau_t(1 + (C_m/C_d))$ (R_1/R_2), $\tau_t = (\tau_0/A_0)$, and $\tau_d = R_dC_d$.

Manuscript received June 21, 1993; revised December 7, 1993.

The authors are with the Luleå University of Technology, S-971 87 Luleå, Sweden.

IEEE Log Number 9216477.

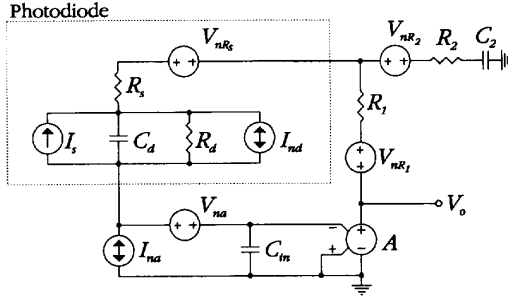


Fig. 3. Noise equivalent circuit of the PIF-circuit. The photodiode noise is represented by I_{nd} and V_{nR_s} , the amplifier noise is represented by I_{na} and V_{na} , and the noise in the feedback network is represented by V_{nR_1} and V_{nR_2} .

TABLE I
PARAMETERS OF THE LINEAR MODEL OF THE IMPLEMENTED PIF-CIRCUIT

R_d	R_s	R_1	R_2	C_d	C_{in}	C_2	A_0	τ_0
150	5 Ω	100 k Ω	82 Ω	8 pF	16 pF	10 μ F	55 \cdot 10 ⁶	7.5 ms

In the derivation of (2), a number of terms have been cancelled due to the conditions below, which are valid for a correctly designed PIF-circuit:

$$A_0 \gg 1 \quad (3)$$

$$\tau_t, R_s C_d \ll \tau_1, \tau_2, \tau_d \quad (4)$$

$$\tau_3 \ll \tau_1, \tau_2 \quad (5)$$

$$R_1 \ll R_d \quad (6)$$

$$R_2 \ll R_1. \quad (7)$$

B. Noise Analysis

A noise equivalent circuit of the PIF-circuit is shown in Fig. 3. The symbols I_{nd} , I_{na} , V_{nR_s} , V_{nR_1} , V_{nR_2} , and V_{na} should be interpreted as the square roots of the spectral densities of the currents and voltages of the respective noise generators.

The total noise of the PIF-circuit is represented by a current noise source connected in parallel with the photocurrent source. With the usual assumption that all noise sources are uncorrelated, the spectral density of the total noise of the PIF-circuit becomes

$$I_{nPIF}^2 = I_{nd}^2 + I_{na}^2 + (V_{nR_s}^2 + k_1 V_{nR_1}^2 + k_2 V_{nR_2}^2 + V_{na}^2) \cdot \left(\frac{1}{R_d^2} + \omega^2 C_d^2 \right) \quad (8)$$

where

$$k_1 = \frac{1 + \omega^2 \tau_2^2}{1 + \omega^2 \tau_1^2} \quad (9)$$

and

$$k_2 = \frac{R_1^2}{R_2^2} \cdot \frac{\omega^2 \tau_2^2}{1 + \omega^2 \tau_1^2}. \quad (10)$$

The function k_2 is approximately equal to one for frequencies well above $1/(2\pi\tau_1)$. This frequency is typically less than 1

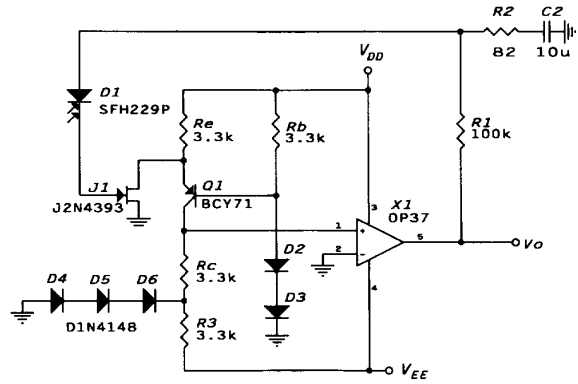


Fig. 4. Circuit diagram of the implemented PIF-circuit. Power supply decoupling components are not shown.

Hz in a correctly designed PIF-circuit. Due to the condition (7), the noise contribution from R_1 is much smaller than the contribution from R_2 throughout the frequency range defined in the Introduction. The expression for the total noise of the PIF-circuit then becomes

$$I_{nPIF}^2 = I_{nd}^2 + I_{na}^2 + (V_{nR_s}^2 + V_{nR_2}^2 + V_{na}^2) \cdot \left(\frac{1}{R_d^2} + \omega^2 C_d^2 \right). \quad (11)$$

IV. AN IMPLEMENTATION OF THE PIF-CIRCUIT

The schematics of an implementation of the PIF-circuit is shown in Fig. 4. The feedback components of the circuit are denoted by R_1 , R_2 , and C_2 . The amplifier consists of the cascode $J1-Q1$ followed by the operational amplifier $X1$.

V. SIMULATIONS

SPICE simulations have been made of the implemented PIF-circuit. Both the linear model, described above, and a complete SPICE model have been used. The parameter values used for the linear model are shown in Table I. The parameters C_{in} , A_0 , and τ_0 are the equivalent input capacitance of the cascode stage, the low-frequency gain, and the time constant of the transfer function of the cascode stage and the operational amplifier.

A. Pulse Response

The pulse responses of the implemented PIF-circuit, given by the linear model and the SPICE model, are shown in Fig. 5. The photocurrent pulse used in the simulations has an amplitude of 10 pA. The rise and fall times of the pulse are 10 μ s and the pulse width is 1 ms.

B. Frequency Response

The magnitudes of the transfer functions using the linear model and the SPICE model are shown in Fig. 6. To illustrate the influence of the photodiode bias point, several curves corresponding to different amounts of dc-current in the photodiode—generated by background light—are shown.

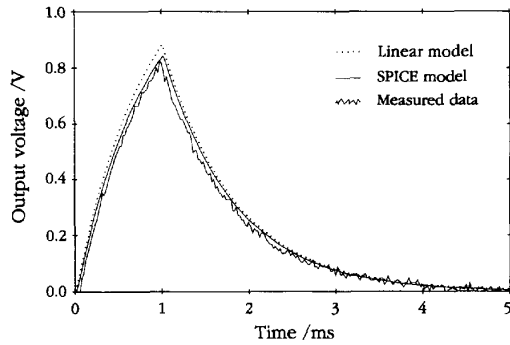


Fig. 5. Pulse response of the implemented PIF-circuit. The amplitude and width of the current pulse in the photodiode are 10 pA and 1 ms, respectively (measured and simulated data).

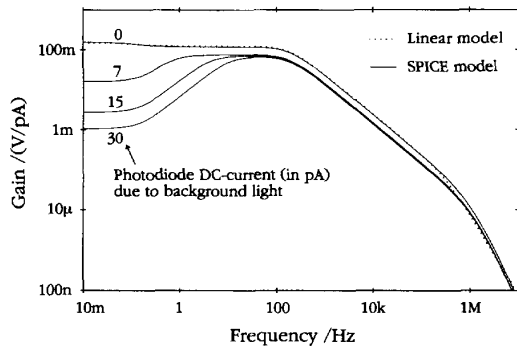


Fig. 6. Magnitudes of the transfer function of the implemented PIF-circuit. The pole given by τ_d and the gain constant of the transfer function are dependent on the bias point of the photodiode. Simulation results.

Both the curve corresponding to the linear model and the curve corresponding to the SPICE model with no background generated dc-current conform well with the derived expression (2) for the transfer function.

C. Noise Properties

The square root of the spectral density of the noise current, given by a SPICE simulation, is shown in Fig. 7. The low-frequency noise is $1.4 \text{ fA}/\sqrt{\text{Hz}}$ and the break frequency is 10 kHz. For comparison, the thermal noise contributions from two fictitious resistors connected in parallel and in series with the photodiode are also shown.

The derived noise expression (11) has been used to calculate the noise properties of the implemented PIF-circuit. The low-frequency noise became $2.0 \text{ fA}/\sqrt{\text{Hz}}$ and the break frequency became 20 kHz. The noise parameters used in the calculations were $I_{nd} = I_{na} = 1.4 \text{ fA}/\sqrt{\text{Hz}}$ and $V_{na} = 2.0 \text{ nV}/\sqrt{\text{Hz}}$.

In this context, a remarkable discovery was made: the shot noise in the gate current of an FET is not modeled in the SPICE model of an FET [4]. The shot noise in the gate current should be approximately equal to the shot noise in the photodiode leakage current because the currents are equal. Then both the simulated low-frequency noise and the simu-

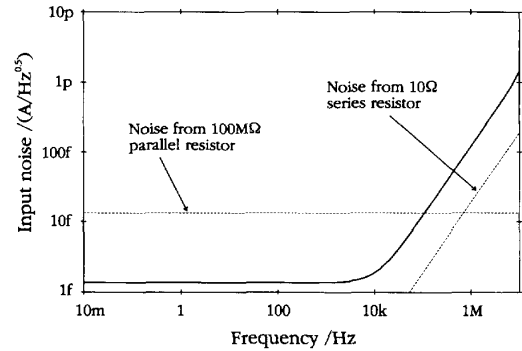


Fig. 7. Input noise of the SPICE model of the implemented PIF-circuit. Noise contributions from a small resistor in series with the photodiode and from a large resistor in parallel with the photodiode are also shown for comparison. Simulation results.

lated break frequency should be scaled by a factor $\sqrt{2}$ to give a correct result. Considering this and the general uncertainties in noise parameters, the calculated noise conforms well with the simulated noise.

VI. MEASUREMENTS

A. Pulse Response

An LED radiating at $\lambda = 650 \text{ nm}$ was used as a light source for the pulse response measurements. The voltage pulse driving the LED was adjusted to produce a current pulse in the photodiode with similar parameters as in the simulations.

The result of the measurement of the pulse response is shown in Fig. 5. Simulated responses, based on the linear model and the SPICE model with no background generated dc-current, are also shown for comparison.

B. Noise Properties

The spectral density of the output noise voltage of the implemented PIF-circuit was measured with a narrow-band spectrum analyzer. The result of the measurements, together with the result from a Monte Carlo simulation based on the SPICE model with no background generated dc-current, are shown in Fig. 8. All SPICE model parameters which have a direct influence on the noise have been given a uniform statistical distribution with a maximum deviation of 50% from their nominal values in the Monte Carlo simulation.

VII. DISCUSSION

A. Transfer Function

Measured pulse response and simulated results using both the linear model and the SPICE model of the implemented PIF-circuit conform well with (2).

For applications with input pulse lengths in the interval 0.1–1 ms, some further simplifications of (2) can be made. In the frequency interval 10 Hz–100 kHz the transfer function

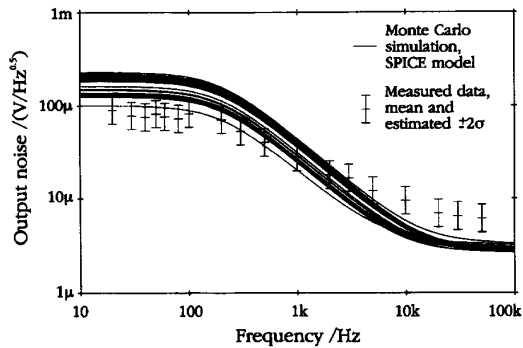


Fig. 8. Output noise of the implemented PIF-circuit. Measured and simulated data.

of the implemented PIF-circuit can be approximated by

$$H_{PIF}(s) \approx \frac{\tau_1}{C_d(1 + s\tau_2)}. \quad (12)$$

An important observation is that R_d has disappeared from the transfer function (12). This is good because the value of R_d is normally poorly known and depends strongly on the photodiode bias point which is ambient light dependent. Although the photodiode junction capacitance C_d is also a function of the photodiode bias point, that dependence is much weaker and is furthermore well known [5]. See Fig. 6.

B. Noise Properties

The expression for the PIF-circuit noise (11) shows that the PIF-circuit has no noise contribution from a load or feedback resistor as other photodiode-amplifier circuits have [1]. Fig. 7 shows the noise contribution from a parallel resistor of 100 M Ω resistance which could be typical for such a resistor.

Also shown in the figure is the noise contribution from a 10 Ω series resistor. This is included to stress the importance of a low series resistance in the photodiode and a low impedance level in the feedback network. The thermal noise in R_s and R_2 contributes to the total noise in the same manner as the amplifier voltage noise.

The measured output noise of the implemented PIF-circuit is less than the predicted noise at frequencies below 1 kHz and larger than the predicted noise above 1 kHz. The discrepancy could possibly be explained by incorrect parameters used in the models of the implemented PIF-circuit. No evidence of $1/f$ -noise has been found in the measurements.

The maximum responsivity of the used photodiode SFH229P is 0.62 A/W at a wavelength of 850 nm. Together with the calculated noise $I_{nPIF} = 2.0 \text{ fA}/\sqrt{\text{Hz}}$ for frequencies below 20 kHz, this gives a corresponding NEP = 3.2 fW/ $\sqrt{\text{Hz}}$ for frequencies below 20 kHz. The measurements indicate that the implemented PIF-circuit has a somewhat lower NEP.

VIII. CONCLUSIONS

A photodiode-amplifier circuit with the photodiode in the feedback path has been presented. It is named the PIF-circuit. The main benefit of the circuit is that it does not need a resistor to provide a path to ground for the signal and leakage currents from the photodiode and the bias current at the amplifier input. Therefore, a strong noise source is eliminated.

A low series resistance in the photodiode and a low impedance level in the feedback network are shown to be important in minimizing the noise of the PIF-circuit.

The PIF-circuit has been used and has shown its performance in several (rocket-borne) instruments built by one of the authors.

REFERENCES

- [1] R. H. Hamstra, Jr., and P. Wendland, "Noise and frequency response of silicon photodiode operational amplifier combination," *Appl. Opt.*, vol. 11, no. 7, pp. 1539-1547, July 1972.
- [2] G. H. S. Rokos, "Optical detection using photodiodes," *Opto-electron.*, vol. 5, pp. 351-366, 1973.
- [3] C. D. Motchenbacher and F. C. Fitchen, *Low-Noise Electronic Design*. New York: Wiley, 1973.
- [4] P. Antognetti and G. Massobrio, *Semiconductor Device Modeling with SPICE*. New York: McGraw-Hill, 1988.
- [5] S. M. Sze, *Physics of Semiconductor Devices*, 2nd. ed. New York: Wiley, 1981.